Plant Cell Tiss Organ Cult (2015) 120:441–451
DOI 10.1007/s11240-014-0611-4

ORIGINAL PAPER

Molecular cloning and identification of an ammonium transporter gene from pear

Hui Li · Yu Cong · Jing Lin · You Hong Chang

Received: 6 April 2014 / Accepted: 28 August 2014 / Published online: 5 September 2014

Abstract The molecular basis of ammonium acquisition in fruit trees remains poorly understood. Here, a new ammonium transporter gene, *PbAMT1;1*, was isolated from *Pyrus betulifolia*. The full length of *PbAMT1;1* was 1,693 bp, coding a protein of 505 amino acids. The deduced structure of the PbAMT1;1 protein revealed 11 membrane-spanning domains and an ammonium transporter signature motif 'D^{204}FAGSGMVHMVGGIAGLWGAFIESPR^{229}', located in the fifth predicted transmembrane region. *PbAMT1;1* transcripts were detectable in all parts of the seedlings and predominantly located to the roots. In addition, a change of pH had little effect on its expression patterns. *PbAMT1;1* expression levels in roots were strongly induced by ammonium depletion and suppressed by high ammonium. However, its transcription levels in leaves were reduced by free nitrogen and increased after high amounts of ammonium were supplying. Further, *PbAMT1;1* exhibited diurnal rhythms with the highest expression at noon. When abscisic acid and methyl jasmonate existed, the mRNA abundance of *PbAMT1;1* increased. The results of yeast complementation showed that the *PbAMT1;1* gene could help yeast mutant stain 31019b to grow in a media with micromole ammonium concentrations. Furthermore, PbAMT1;1 mediated NH_4^+ uptake with high affinity producing K_m values from 20.9 to 23.2 μM at different pH values. However, the net $^{15}NH_4^+$ uptake K_m of PbAMT1;1 showed no significant differences at pH 4.8, 5.8 or 6.8. In conclusion, *PbAMT1;1* is a functional *AMT* gene having the features of the AMT1 family. Its expression was regulated by ammonium concentration, diurnal rhythms and plant hormones, but not by external pH levels.

Keywords *Pyrus betulifolia* · Ammonium transporter · Functional characterization · Regulation

Abbreviations

AMT	Ammonium transporter
MeJ	Methyl jasmonate
MES	2-(*N*-morpholino) ethanesulfonic acid
N	Nitrogen
NCBI	The National Center for Biotechnology Information
ORF	An open reading frame
p*I*	Isoelectric point
RACE	Rapid amplification of cDNA ends
TM	Transmembrane domains
UTR	Untranslated region

Introduction

As an important nutrient and ubiquitous intermediate in plant nitrogen (N) metabolism, ammonium, NH_4^+, is mainly transported and distributed by a family of integral membrane proteins known as ammonium transporters (AMTs). According to phylogenetic relationships, plant

Hui Li and Yu Cong have contributed equally to this work.

H. Li · J. Lin · Y. H. Chang (✉)
Institute of Horticulture, Jiangsu Academy of Agricultural Sciences/Jiangsu Key Laboratory for Horticultural Crop Genetic Improvement, Nanjing, China
e-mail: jaaschang@163.com

Y. Cong
State Key Laboratory of Soil and Sustainable Agriculture, Institute of Soil Science, Chinese Academy of Sciences, Nanjing, China

AMTs can be subdivided into AMT1 and AMT2 subfamilies (Loqué and von Wirén 2004). Compared with the AMT2 subfamily, the functionality of the AMT1 subfamily has been studied more extensively. Since the first plant *AMT1* gene was identified from *Arabidopsis* by functional complementation of a yeast mutant defective in high-affinity ammonium uptake (Ninnemann et al. 1994), many homologues have been isolated from different species, such as tomato (Lauter et al. 1996; von Wirén et al. 2000), *Arabidopsis* (Sohlenkamp et al. 2000; Yuan et al. 2009), rice (Kumar et al. 2003; Sonoda et al. 2003; Yamaya et al. 2003), lotus (D'Apuzzo et al. 2004; Guether et al. 2009; Salvemini et al. 2001; Udvardi et al. 2003), *Citrus* (Camanẽs et al. 2007) and poplar (Couturier et al. 2007).

The members of the AMT1-type family presumably carry out discrete, though perhaps partially overlapping roles in plants (D'Apuzzo et al. 2004). Many studies on the model plant *A. thaliana* showed that three ammonium transporters (AtAMT1;1, AtAMT1;2 and AtAMT1;3) were responsible for ~90 % of the total high affinity uptake in roots (Yuan et al. 2007). In addition, another AMT1 homologue AtAMT1;4 has roles in other organs, such as pollen and pollen tubes (Yuan et al. 2009). It is interesting that the AMT1-type homologous genes have their own regulatory characteristic when plants are subjected to different N regimes. For example, transcript levels of *AtAMT1;1* of *Arabidopsis* were up-regulated, while *AtAMT1;2* was not significantly induced by N deprivation in roots (Shelden et al. 2001). Moreover, the transcript abundance of maize *ZmAMT1;1a* and *ZmAMT1;3* (Gu et al. 2013), rice *OsAMT1;1* and *OsAMT1;2* (Sonoda et al. 2003) decreased during N starvation periods. *AMT* genes from different species show multiple expression patterns, which suggests that, although AMTs were characterized in detail from various species, it is necessary to characterize homologous AMTs from species that are the subject of more applied research.

Until now, lots of knowledge of AMT1 was focused on herbs. With the exceptions of poplar (Couturier et al. 2007) and *Citrus* AMT1s (Camanẽs et al. 2007, 2009), little is known about AMTs from woody plants. Pear is an economically important tree in China, and grafting of elite cultivars (scions) onto rootstocks is an efficient approach to improving fruit production. *Pyrus betulifolia* is native to China and is used widely as a rootstock for pear cultivation (Okubo and Sakuratani 2000). After grafting onto this rootstock, pear trees are more tolerant to high humidity, drought, flooding and salt stress (Kaneyoshi et al. 2001; Matsumoto et al. 2006; Okubo and Sakuratani 2000). Despite the great importance of *P. betulifolia* as a pear rootstock, which absorbs N from the soil and transports it to shoots (the scion), the ammonium transport system in *P. betulifolia* remains poorly understood. In this study, a *P. betulifolia* AMT1-type ammonium transporter has been isolated and its transcriptional regulation characterized under different ammonium concentrations. A parallel analysis of the yeast complementation effects of *PbAMT1;1*, as well as $^{15}NH_4^+$ contents in recombinant yeast cells, allowed us to address regulatory features of the gene function in response to protons. This work offers a preliminary understanding of the ammonium transporter features of the *PbAMT1;1* gene from *P. betulifolia* plants.

Materials and methods

Plant material and treatments

Mature seeds of *P. betulifolia* were collected from Shankou Town, Taian City, Shandong Province, China, in November 2012. After being stratified for 40 days, seeds were planted in pots with quartz sand. The nutrient solution, buffered with 0.2 % (w/v) MES, which contained 0.75 mM $CaCl_2{\cdot}2H_2O$, 4.7 mM KCl, 2.5 mM NH_4Cl, 0.375 mM $MgSO_4{\cdot}7H_2O$, 0.3 mM KH_2PO_4, 100 μM H_3BO_3, 5 μM KI, 100 μM $MnSO_4{\cdot}H_2O$, 30 μM $ZnSO_4{\cdot}H_2O$, 1 μM $Na_2{\cdot}Mo_4{\cdot}2H_2O$, 0.1 μM $CuSO_4{\cdot}5H_2O$, 0.1 μM $CoCl_2$, 100 μM $FeSO_4{\cdot}7H_2O$ and 100 μM $Na_2EDTA{\cdot}2H_2O$, was added to the pots every 3 days until the seedlings' second true leaf fully expanded. Then, uniform seedlings were transferred to the hydroponic system in an illuminating growth incubator at 23 °C, with 70 % relative humidity, 300 μmol m^{-2} s^{-1} light intensity and a 16/8 h light/dark period. The components of the nutrient solution were as above and renewed every 3 days to keep the pH at 5.8. At the same time, an air pump was used to maintain good air circulation. When seedlings were 30 days old, they were collected for treatments.

RNA and DNA work

Total RNA was extracted from leaf, stem and root samples with the StarSpin Plant RNA Mini Kit (GenStar, China), according to the manufacturer's instructions. Then, RNA samples were treated with DNase I (GenStar, China) to eliminate genomic DNA contamination. An M-MLV RTase cDNA Synthesis Kit (TaKaRa, Japan) was used to obtain first-strand cDNA from purified total RNA. At the same time, genomic DNA was extracted using the Plant Genomic DNA Kit (Tiangen, China).

Isolation of full-length cDNAs and DNA sequences

The amino acid sequence of AtAMT1;1 (NCBI accession no. CAA53473) from *A. thaliana* was employed as an electronic probe to retrieve expressing sequence tags (ESTs) from the

Malus database of NCBI by means of tblastn. Then, four ESTs (DT043026, DR991055, DT000749 and CO415539) containing the initiator codon 'ATG' were selected from several related ESTs, and were used as 5′ template sequences for designing PCR primers. Finally, a pair of primers [(5′-CACCTCTCTTCTTTCTCTCTCTA-3′, forward primer) and (5′-TCGGCAATGGATCCGCTGGT GATTC-3′, reverse primer)] was used to amplify the corresponding sequence in *P. betulifolia*, which has a relatively close relationship to *Malus*.

To obtain the full length cDNA sequences, the gene-specific primers (GSP: 5′-CTGGCTCCGTCCGCGCA AAGAACACC-3′ and NGSP: 5′-GAATCACCAGCG GATCCATTGCCGA-3′) were designed according to 5′ fragment sequencing results. Furthermore, 3′-RACE was performed using a SMART™ RACE cDNA Amplification Kit (Clontech, Japan). Finally, CAP3 (http://pbil.univ-lyon1.fr/cap3.php) was used to ligate the 5′-region and 3′-RACE sequences together to obtain the full length gene. In addition, ORF was located using the online server program ORF finder (http://www.ncbi.nlm.nih.gov/gorf/gorf.html) (Wang et al. 2013). Based on the results, high fidelity PCR amplification (PrimeSTAR® HS DNA Polymerase, TaKaRa, Japan) was performed to isolate the ORF sequence via the primers [(5′-ATGGCGACGTGGGCAACACTA GACTG-3′, forward primer) and (5′-CTAAACA GACGGGGGCGTGGACGAAG-3′, reverse primer)]. All PCR products were purified using an Agarose Gel DNA Purification Kit Ver.2.0 (TaKaRa, Japan) and sequenced. The corresponding genomic sequence was obtained similarly using genomic DNA as the PCR template.

Bioinformatics analysis

The theoretical p*I* and mass values for mature peptide were calculated using the PeptideMass program (http://us.expasy.org/tools/peptide-mass.html) (He et al. 2013). Transmembrane regions and subcellular localization were predicted by TMHMM Server v. 2.0 (http://www.cbs.dtu.dk/services/TMHMM/) and the Wolf PSORT (http://wolfpsort.org/), respectively. The AMT signature motif was determined with ScanProsite tools at ExPaSy (http://expasy.org/tools/ scanprosite/). The C-terminal phosphorylation sites were predicted with NetPhos 2.0 Server (http://www.cbs.dtu.dk/services/NetPhos/). In order to compare the homologous among various AMT1 proteins, an alignment was performed using CLC Sequence Viewer 6 software. Full-length amino acid sequences were aligned by ClustalW and imported into the Molecular Evolutionary Genetics Analysis (MEGA) package version 5.01 (Tamura et al. 2011). Then, the neighbor-joining method was applied for phylogenetic analyses in MEGA. Bootstrap tests were conducted using 1,000 replicates, and the branch lengths are proportional to the phylogenetic distances.

Real-time PCR quantification analysis

A set of PCR primers [(5′-ACTTGATCCAGATAGTGG T-3′, forward primer) and (5′-GACGAAGT GTTCGGCTCGA-3′, reverse primer)], which yielded an amplicon of 226 bp, was designed for quantitative real-time RT-PCR (qPCR). The *Pbactin* gene was used simultaneously as a housekeeping gene (Chang et al. 2012). qPCR was performed on BIO-RAD CFX96 Real-Time PCR Detection Systems (Bio-Rad, USA) with SYBR® Premix Ex Taq™ (TaKaRa, Japan). The PCR mixture (25 μL total volume) contained 12.5 μL 2 × SYBR® Premix Ex Taq™ (TaKaRa, Japan), 0.5 μL of each primer (10 μM), 2 μL of tenfold diluted cDNA and 9.5 μL ddH_2O. The PCR program was initiated at 95 °C for 30 s, followed by 40 cycles of 95 °C for 5 s, 57 °C for 30 s, and 72 °C for 30 s, and completed with a melting curve analysis program. No-template blank controls were included in every reaction batch. After PCR, qPCR products were run in 2.0 % agarose gels, stained with ethidium bromide and photographed to ensure their size in accordance with expectation.

Yeast growth, transformation and complementation

The yeast expression vector of pYES2-PbAMT1;1 was constructed by cloning the *PbAMT1;1* ORF into the pYES2 vector (Invitrogen, USA). The yeast mutant strain 31019b (*Δmep1*, *Δmep2*, *Δmep3* and *ura3*), which is unable to grow on medium containing <5 mM NH_4^+ as the sole N source (Marini et al. 1997) was kindly provided by Professor Nicolaus Von Wirėn (Leibniz-Institute for Plant Genetics and Crop Plant Research, Gatersleben, Germany). Yeast cells were transformed with pYES2-PbAMT1;1 plasmid by electroporation (MicroPulser, Bio-Rad, USA). Transformants were selected and further isolated on solid YNB (minimal yeast growth medium without amino acids or ammonium sulfate, Difco, USA) medium supplemented with 1 mM arginine and 2 % galactose. Overnight cultures from single colonies with equal cell densities were serially diluted by factors of 10, and 5 μL of each dilution was spotted on YNB medium plates supplemented with NH_4^+ as the sole N source for complementation testing. Cells were grown at 30 °C for 3 days and documented by scanning the plate in the grayscale mode using the Tanon-3500 digital gel imaging system (Tanon Science & Technology, China).

$^{15}NH_4^+$ uptake assays

The recombinant yeast cell colonies were grown in a liquid arginine medium until the OD_{600} reached approximately 0.5–0.6. Cells were harvested, washed and re-suspended in an uptake buffer (100 mM sodium phosphate buffer, pH 4.8, 5.8 or 6.8) to a final OD_{600} of 40. Before uptake, cells were energized by adding 100 μL 4 % galactose to 200 μL cells and incubated for 12 min at 30 °C. Uptake was initiated by adding 300 μL uptake buffer containing $^{15}NH_4^+$ (≥98.5 atom % ^{15}N, Shanghai Research Institute Of Chemical Industry, China). After that, cells were incubated in a shaker at 30 °C, 220 rpm. Then, cells were immediately transferred on ice for 20 s, and centrifuged for 20 s to form pellets and to discard the tracer solution. Afterwards, cells were washed three times in 1 mL of ice-cold buffer, followed by 20 s of centrifugation for each wash. After the last wash, cell pellets were frozen at −80 °C for 10 min, and then cells were dried at 65 °C for 72 h. Approximately 500 ng of homogenized cell powder was subjected to total N content and $^{15}N/^{14}N$ ratio measurements using an elemental analyzer with an isotope ratio mass spectrometer (Flash EA 2000-ConfloIV-Delta V ADVANTAGE, Thermo Finnigan, USA). The absorption rate of ^{15}N was calculated according to the formula: [Total N content × ($^{15}N/^{14}N$ − 0.366)]/(Molecular weight of ^{15}N × Treatment time).

Statistical analysis

Data from at least three independent experiments were analyzed by one-way ANOVA using Sigmaplot v11.0 (Jandel Scientific Software, San Rafael, CA, USA), and the differences were compared by the Duncan test with a significance level of $P < 0.05$.

Results

Gene isolation and sequence analysis of *PbAMT1;1*

After the publishing of EST data, EST database mining becomes an effective means for obtaining new genes. Since

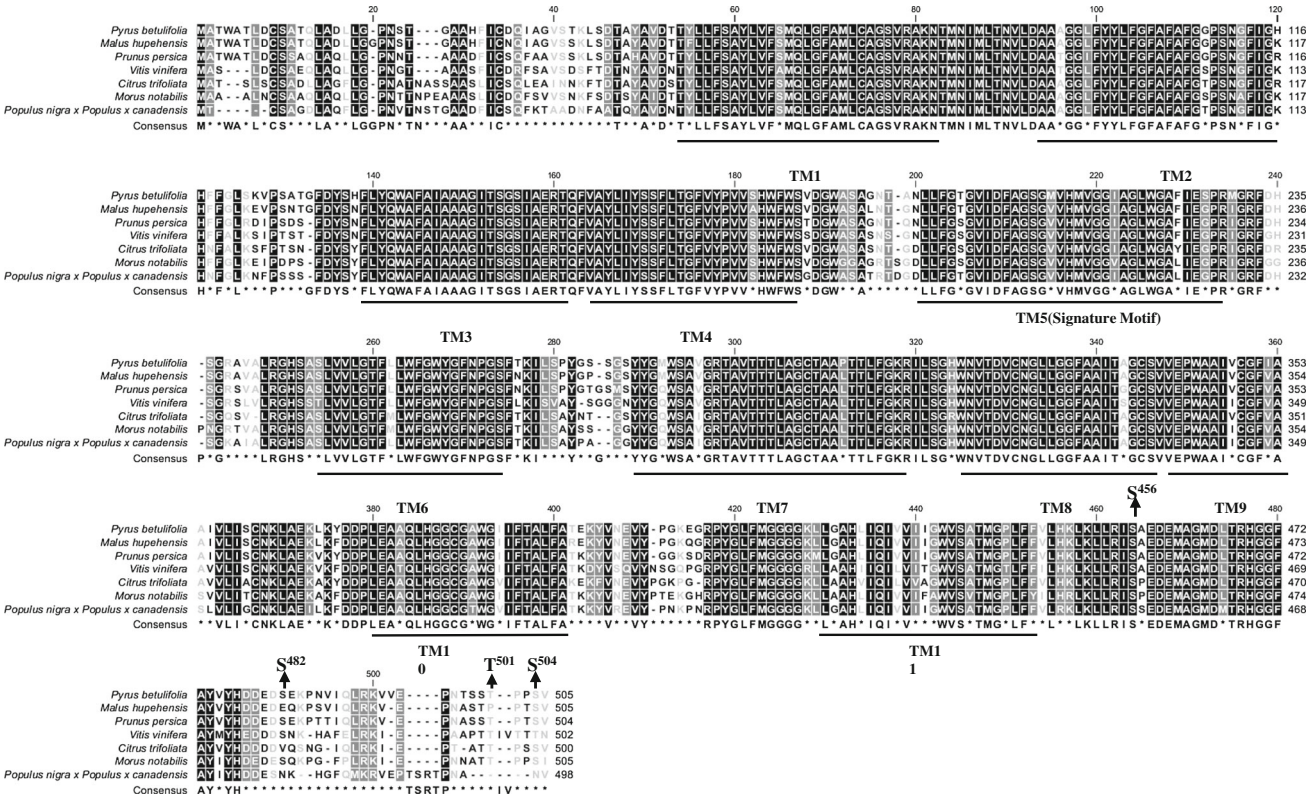

Fig. 1 Alignment of *PbAMT1;1* deduced amino acid sequences with closely related AMTs. Alignment was conducted with CLC Sequence Viewer 6 software. TMs were predicted using the TMHMM Server (http://www.cbs.dtu.dk/services/TMHMM/). The AMT signature motif was determined with the ScanProsite tools at ExPaSy (http://expasy.org/tools/scanprosite/). Identical residues are shown in *black*, gaps are indicated as *asterisks*, predicted TM are outlined by *thick lines* on *bottom*, and the signature motif is marked by the *bracket*, phosphorylation sites are indicated by *up arrow*. *P. betulifolia*, PbAMT1;1, AHJ60273; *Malus hupehensis*, MhAMT1;1, AEY75246; *Prunus persica*, hypothetical protein PRUPE_ppa004542 mg, XP_007223306; *Citrus trifoliate*, CtrAMT1;1, AFO66660; *Morus notabilis*, MnAMT1;1, EXB95961; *Vitis vinifera*, VvAMT1;1, XP_002285558; *Populus nigra x Populus Canadensis*, PnpcAMT1;1. AHA42545

Pyrus has a close genetic relationship with *Malus*, a 496 bp fragment of the 5′ sequence, which was similar to the *AMT* gene, was isolated from *P. betulifolia* according to the EST sequences information of *Malus*. Then, a 1,222 bp cDNA sequence, including an 18 bp poly-A tail, was obtained via 3′-RACE. By joining these two cDNA sequences, we gained a 1,693 bp sequence, which contained a 1,518 bp ORF, 32 bp 5′ UTR and 143 bp 3′ UTR between the "TAG" stop codon and the putative terminal poly-A tail. Finally, one high-fidelity PCR was carried out to verify the overlapping sequence. The PCR product (named as *PbAMT1;1*, NCBI accession no. KJ123648) matched the above sequence perfectly, which supported our sequence selection. In addition, the DNA sequence of *PbAMT1;1* was consistent with its cDNAs, which indicated that *PbAMT1;1* has no intron in its ORF.

PbAMT1;1 encodes a polypeptide of 505 amino acids, which has the p*I* and mass values of 6.87 and 53.8 kDa, respectively. Based on structural predicted results, PbAMT1;1 was a membrane protein located on the plasma membrane. PbAMT1;1 had 11 TMs (Fig. 1), with a hydrophilic amino-terminus and carboxyl-terminus located extracellularly and in the cytoplasm, respectively. These features conform to the predicted prototype of AMT proteins. It is worth noting that in the fifth transmembrane helix (Fig. 1) there was a motif, 'D^{204}FAGSGMVHMVGGIAGLWGAFIESPR^{229}', that corresponded to D-[FYWS]-[AS]-G-[GSC]-x(2)-[IV]-x(3)-[SAG](2)-x(2)-[SAG]-[LIVMF]-x(3)-[LIVMFYWA](2)-x-[GK]-x-R, which is generally considered as the hallmark of a potential AMT (de Castro et al. 2006). There are four predicted phosphorylation sites in the C terminus of the PbAMT1;1 protein, which included three serine (Ser^{456}, Ser^{482} and Ser^{504}) sites and one threonine (Thr^{501}) site (Fig. 1). These putative phosphorylation sites may allow for the post-transcriptional regulation of the transporter.

Sequence alignment and phylogenetic analysis

A multiple sequence alignment of eight plant AMT1 proteins revealed that they shared a very high similarity amongst the 11 TMs, especially the signature motif on the fifth TM (Fig. 1). Moreover, the putative amino acid sequence of *PbAMT1;1* shared a high similarity with the other AMT1;1 proteins of ligneous species, such as *Citrus* CitAMT1 (82.48 %) and *Malus* MhAMT1;1 (75.72 %).

To analyze the phylogenetic relationship between PbAMT1;1 and AMT proteins from 12 other representative plants, full length amino acid sequences were aligned by ClustalW and imported into the MEGA package version 5.01 (Tamura et al. 2011). The phylogenetic tree showed that plant AMTs were divided into two subfamilies and PbAMT1;1 belonged to the AMT1 family (Fig. 2).

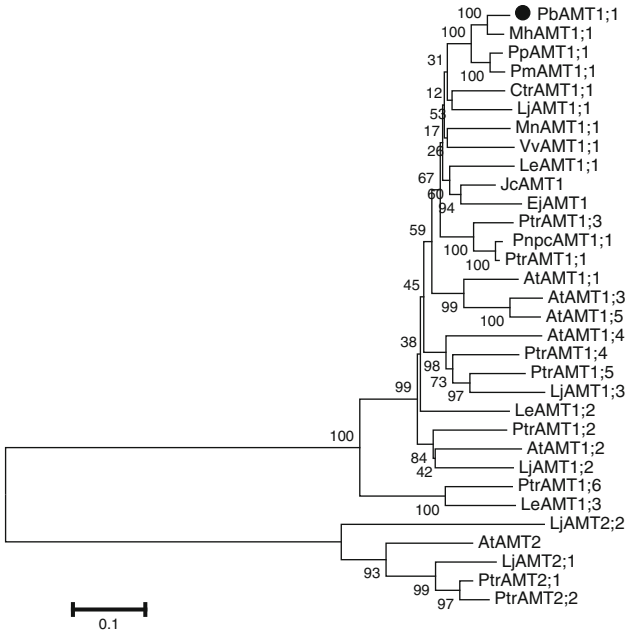

Fig. 2 An unrooted, neighbor-joining (NJ)-based tree of the ammonium transporter family. The dendrogram was generated by Mega 5.01 software using ClustalW for the alignment and the neighbor-joining algorithm with a total of 1,000 bootstrap replicates. The *bottom bar* length represents 0.1 substitutions per amino acid. AtAMT1;1, AtAMT1;2, AtAMT1;3, AtAMT1;4, AtAMT1;5 and AtAMT2 from *A. thaliana* (NCBI accession no. CAA53473, AAD54639, AAD54638, CAB81458, NP_189072 and NP_181363); CtrAMT1 from *Citrus sinensis x Poncirus trifoliate* (DQ887678); EgAMT1 from *Eucalyptus grandis* (KCW60162); JcAMT1 from *Jatropha curcas* (KDP33351); LeAMT1;1, LeAMT1;2 and LeAMT1;3 from *Lycopersicon esculentum* (X92854, CAA64475 and Q9FVN0); LjAMT1;1, LjAMT1;2, LjAMT1;3 and LjAMT2;1 from *Lotus japonicas* (AAG24944.1, AY135020, AJ575588 and AF187962); MhAMT1;1 from *M. hupehensis* (JQ072026); MnAMT1;1 from *M. notabilis* (EXB95961); PbAMT1;1 from *P. betulifolia* (KJ123648); PnpcAMT1;1 from *P. nigra x P. canadensis* (AHA42545); PpAMT1;1 from *P. persica* (XP_007223306); PmAMT1;1 from *Prunus mume* (XP_008224012); PtrAMT1;1, PtrAMT1;2, PtrAMT1;3, PtrAMT1;4, PtrAMT1;5, PtrAMT1;6, PtrAMT2;1 and PtrAMT2;2 from *P. trichocarpa* (XM_002314482, XM_002325754, XM_002311667, XM_002303068, XM_002301801, XM_002314070, XM_002309115 and XM_002323564); VvAMT1;1 from *V. vinifera* (XP_002285558)

Furthermore, PbAMT1;1 was most related to MhAMT1;1 from *Malus* (NCBI accession no. ABI52423) (Fig. 2).

Expression patterns of *PbAMT1;1*

To obtain the preliminary indication of physiological function, the abundance of *PbAMT1;1* transcripts was investigated in root, stem, and leaf tissues of *P. betulifolia* seedlings. Total RNA was used as the template in qPCR to determine if a DNA residual existed. No amplification occurred, indicating that the RNA was not contaminated with DNA (data not shown).

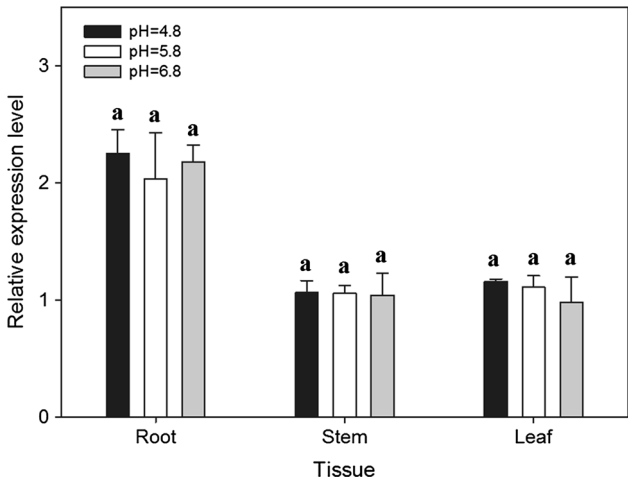

Fig. 3 *PbAMT1;1* expression in different tissues of seedlings under normal N supply at different pH values. 30-day old *P. betulifolia* seedlings were subjected to different pH values treatments for 3 days (pH values were adjusted by 5 M NaOH). The *PbAMT1;1* transcript level was normalized to the expression of *Pbactin* measured in the same samples. Each *bar* represents the average data with standard error of three independent experiments. *Different letters* indicate significant differences ($P < 0.05$)

At the seedling stage, *PbAMT1;1* is more highly expressed in roots than in leaves or in stems under normal growth conditions (Fig. 3). Different pH values had little effect on the expression patterns (Fig. 3). Furthermore, the transcript levels were analyzed after seedling treatments with different N concentrations. *PbAMT1;1* transcripts strongly increased in roots under a short period of N starvation (~3.5-fold at 24 h), but declined after 48 h of N starvation and returned to a normal level at 72 h (Fig. 4a). Finally, its transcriptional level in roots increased again upon N resupply (Fig. 4a). It is worth noting that the expression of *PbAMT1;1* in stem and leaf tissues was only affected by N starvation, but not by N resupply (Fig. 4b, c), whereas in leaves and stems, expression levels of *PbAMT1;1* continued to decline during N starvation (Fig. 4b, c).

When high ammonium (10 mM) was used to treat the seedlings, *PbAMT1;1* transcripts were strongly suppressed in roots and stems (Fig. 5a, b), in contrast, expression of *PbAMT1;1* in leaves increased (Fig. 5c). The *PbAMT1;1* expression pattern suggested that this gene may play a role as an ammonium uptake transporter from the roots to the shoots and would be regulated by ammonium status.

The diurnal variations in *PbAMT1;1* expression levels in leaves were also studied in this work. It was indicated that *PbAMT1;1* exhibited diurnal rhythms with the highest expression at noonday (Fig. 6). Through this photoperiodicity, we may conclude that *PbAMT1;1* plays a limited role in the transportation of NH_4^+/NH_3 generated by photorespiration.

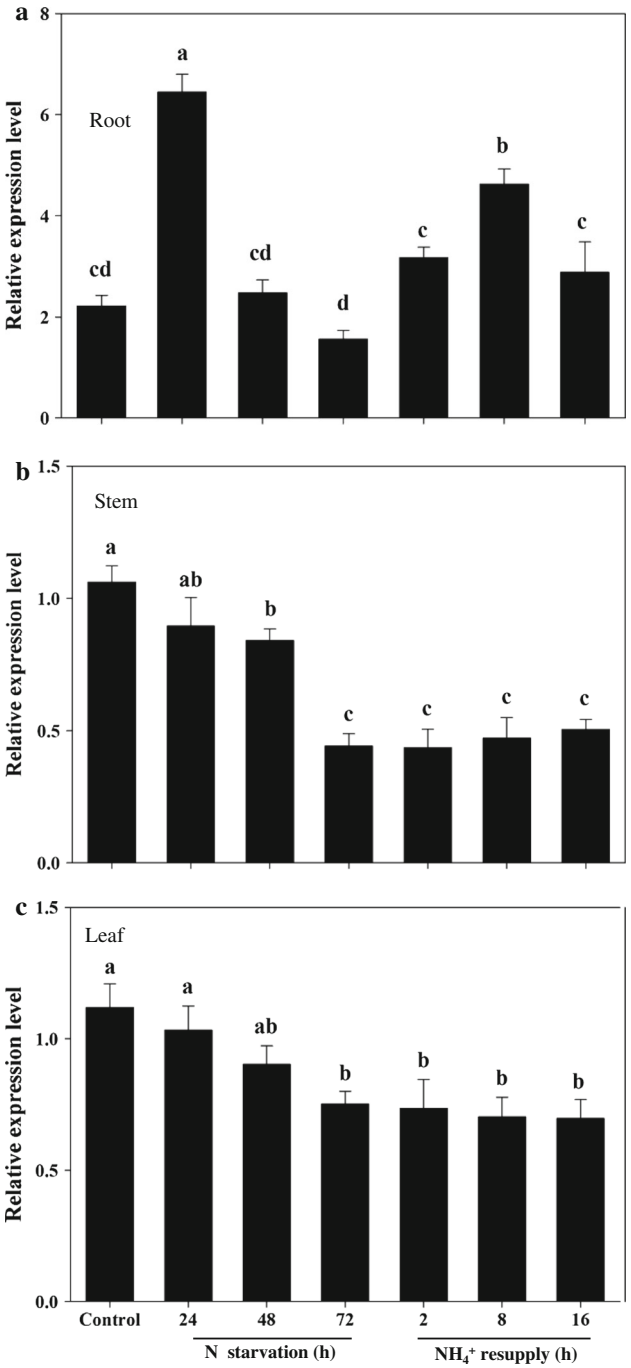

Fig. 4 *PbAMT1;1* expression in roots, stems and leaves during N starvation and resupply. 30-day old *P. betulifolia* seedlings were subjected to different NH_4^+ treatments at indicated time periods. For N starvation treatment, 2.5 mM NH_4Cl in the nutrient solution (see "Materials and methods" section) was replaced by same millimolar of NaCl. After 72 h, the nutrient solution was renewed, which did not change any ingredients, as N resupply treatment. The *PbAMT1;1* transcript level was normalized to the expression of *Pbactin* measured in the same samples. Each *bar* represents the average data with standard error of three independent experiments. *Different letters* indicate significant differences ($P < 0.05$). **a**–**c** *PbAMT1;1* expression in roots, stems and leaves during N starvation and NH_4^+ resupply, respectively

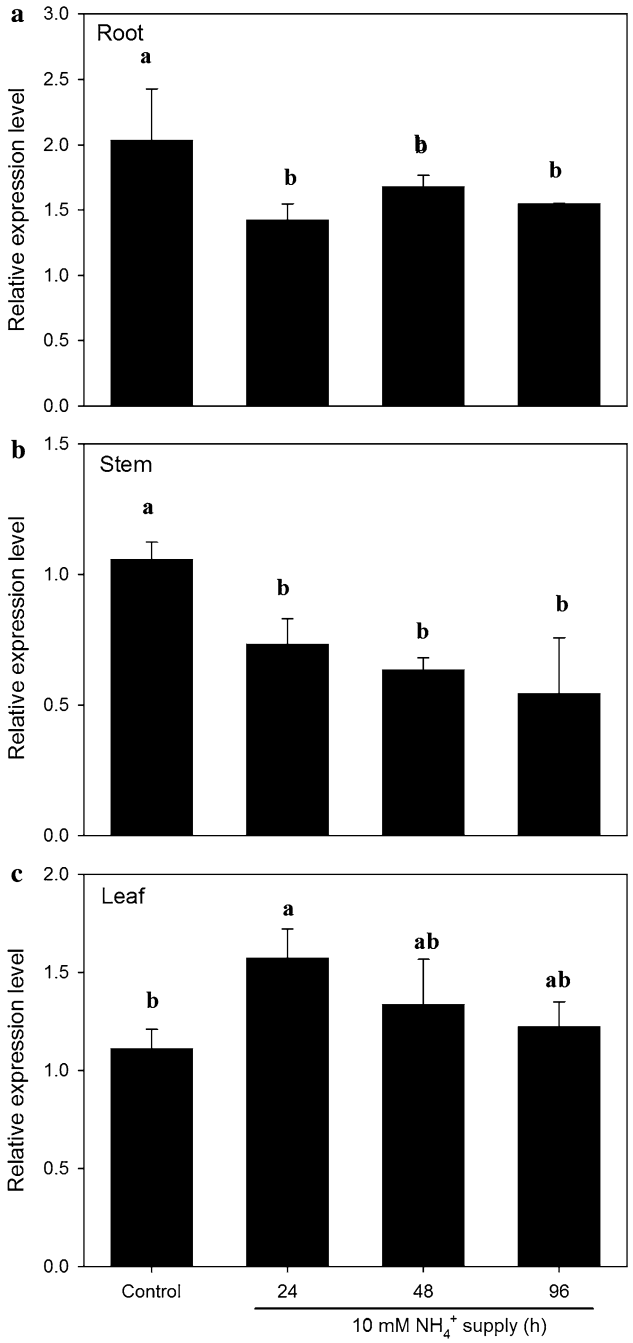

Fig. 5 *PbAMT1;1* expression in roots, stems and leaves under high ammonium. 30-day old *P. betulifolia* seedlings were subjected to high NH_4^+ treatments (10 mM) at indicated time periods. 2.5 mM NH_4Cl in the nutrient solution (see "Materials and methods" section) was replaced by 10 mM NH_4Cl. The *PbAMT1;1* transcript level was normalized to the expression of *Pbactin* measured in the same samples. Each *bar* represents the average data with standard error of three independent experiments. *Different letters* indicate significant differences ($P < 0.05$). **a**–**c** *PbAMT1;1* expression in roots, stems and leaves, respectively

In the presence of ABA and MeJ, the transcription of *PbAMT1;1* increased (Fig. 7). Because both ABA and MeJ can induce the senesce of leaves, we speculated that

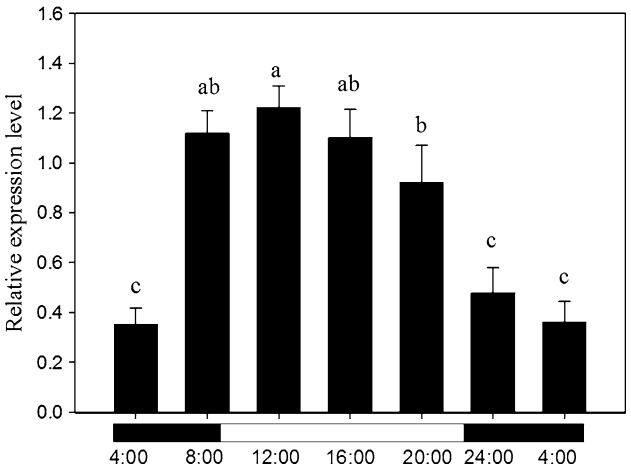

Fig. 6 Effect of the light–dark cycle on *PbAMT1;1* expression in leaves. 30-day old *P. betulifolia* seedlings were cultured in an illuminating growth incubator with a 16 h (8:00 ~ 24:00)/8 h (0:00 ~ 8:00) light/dark period. The *PbAMT1;1* transcript level was normalized to the expression of *Pbactin* measured in the same samples. Each *bar* represents the average data with standard error of three independent experiments. *Different letters* indicate significant differences ($P < 0.05$)

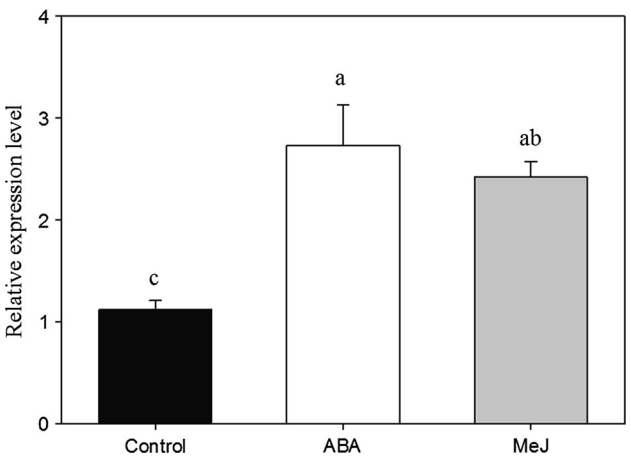

Fig. 7 Effect of the ABA or MeJ on *PbAMT1;1* expression in leaves. 30-day old *P. betulifolia* seedlings were subjected to 100 μM ABA or 100 μM MeJ in the normal nutrient solution (see "Materials and methods" section). The *PbAMT1;1* transcript level was normalized to the expression of *Pbactin* measured in the same samples. Each *bar* represents the average data with standard error of three independent experiments. *Different letters* indicate significant differences ($P < 0.05$)

PbAMT1;1 may be involved in the N backflow in the autumn.

Functional expression of *PbAMT1;1* in yeast

A complementation experiment was carried out to reveal the function of *PbAMT1;1*. The yeast strain 31019b is defective in NH_4^+ transporters and is unable to grow on

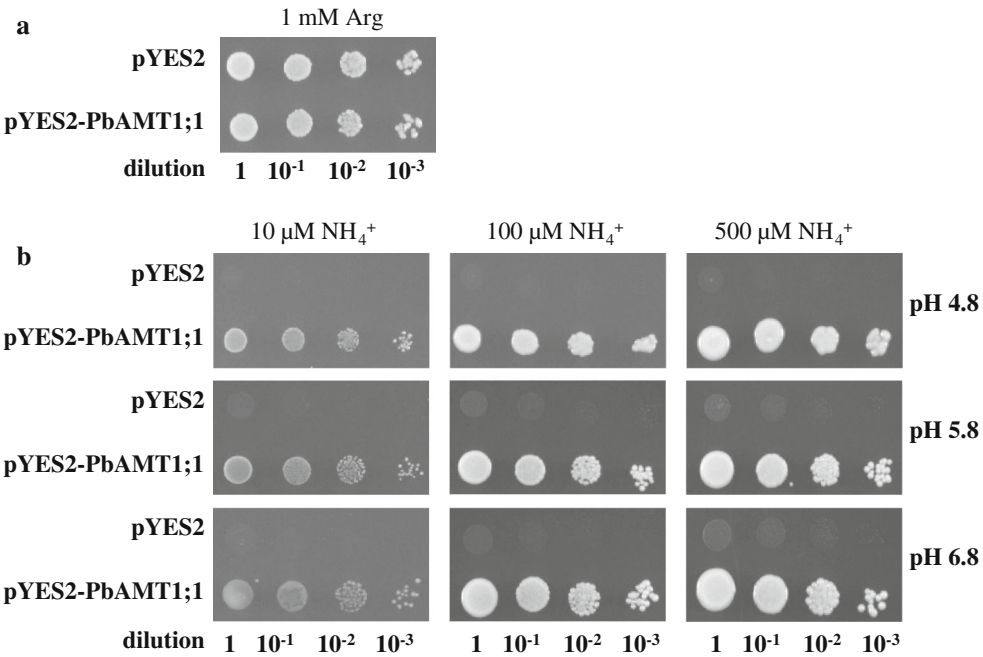

Fig. 8 Complementation of yeast mutant strain 31019b by *P. betulifolia* ammonium transporter *PbAMT1;1* gene. Yeast strain 31019b was transformed with the yeast expression vector pYES2 harboring the *PbAMT1;1* ORF sequence (pYES2-PbAMT1;1). The strain pYES2 (transformation with the yeast expression vector pYES2) was used as the negative control. Growth was assayed on minimal medium containing different sole nitrogen source. **a** 1 mM Arg at pH 5.8, **b** 10, 100 or 500 μM ammonium at pH 4.8, 5.8 or 6.8, respectively. Serial dilutions of cell suspensions ranged from 1 to 1×10^{-3}. Pictures were taken after 3 days of growth at 30 °C

medium containing less than 5 mM NH_4^+ as the sole N source (Marini et al. 1997). The results showed that the recombinant yeast strain pYES2-PbAMT1;1 (31019b transformed with the yeast expression vector pYES2 carrying the *PbAMT1;1* ORF sequence under the control of the pGAL1 promoter) and control strain pYES2 (31019b transformed with the yeast expression vector pYES2) both returned to normal growth on 1 mM arginine medium, indicating that the vector's construction and the yeast activity were satisfactory (Fig. 8a). Moreover, the recombinant pYES2-PbAMT1;1 conferred to 31019b the ability to grow with 10–500 μM NH_4^+ as the sole N source (Fig. 8b). As a negative control, carrying pYES2 yeast cells could not grow (Fig. 8b). The above phenomenon indicate that PbAMT1;1 works in mediating active ammonium transport.

At the same time, a set of ^{15}N-labelled uptake experiments were carried out to assess the kinetic properties of PbAMT1;1. When $^{15}NH_4^+$ was in the range of 10–500 μM and the pH was 4.8, 5.8 or 6.8, the $^{15}NH_4^+$ influx in strains containing pYES2 followed almost an unsaturated linear concentration dependency, while the $^{15}NH_4^+$ influx in strains containing pYES2-PbAMT1;1 were saturated at approximately 100 μM (Fig. 9a, c, e). The net $^{15}NH_4^+$ influxes of different pH values mediated by the PbAMT1;1 protein were then determined, which fitted a saturable Michaelis–Menten kinetics with K_m values of ~21.5, ~23.2 and ~20.9 μM, respectively (Fig. 9b, d, f), which represented no significant differences. This result indicated that PbAMT1;1 was a high-affinity AMT. In addition, the net $^{15}NH_4^+$ uptake K_m of the pYES2-PbAMT1;1 yeast cells showed no significant differences at pH 4.8, 5.8 and 6.8 (Fig. 10), which supported the view that the uptake ability of PbAMT1;1 was not affected by external pH values.

Discussion

For first time, the cDNA and DNA of the *PbAMT1;1* gene have been isolated from the pear rootstock *P. betulifolia* and shown to have potential roles in the influx of NH_4^+. The deduced amino acid sequence of *PbAMT1;1* contains a hallmark motif of a potential AMT in the fifth transmembrane helix (Fig. 1), and it has high homology with other *AMT1* genes (Fig. 2). Furthermore, this gene transcript levels were changed in response to N starvation, N resupplies, high ammonium treatment, photoperiod and plant hormones (Figs. 4, 5, 6, 7). Finally, *PbAMT1;1* could help the yeast strain 31019b to return to normal growth when 10–500 μM NH_4^+ as the sole N source (Fig. 8). Thus, we concluded that *PbAMT1;1* corresponds to the *AMT1* gene.

The present data indicated that the *PbAMT1;1* expression pattern was similar to that of *CitAMT1* from *Citrus* and *AtAMT1;1* from *Arabidopsis*. All of these genes are expressed in all vegetative organs, but predominantly in roots (Shelden et al. 2001, Camanẽs et al. 2007, Fig. 3). However, the regulation modes of *PbAMT1;1* transcripts under different N regimes were different in the roots and aerial plant parts (Fig. 4). In roots, the *PbAMT1;1* transcript was drastically up-regulated once N starvation and N resupply occurred (Fig. 4a). Thus, we hypothesize that

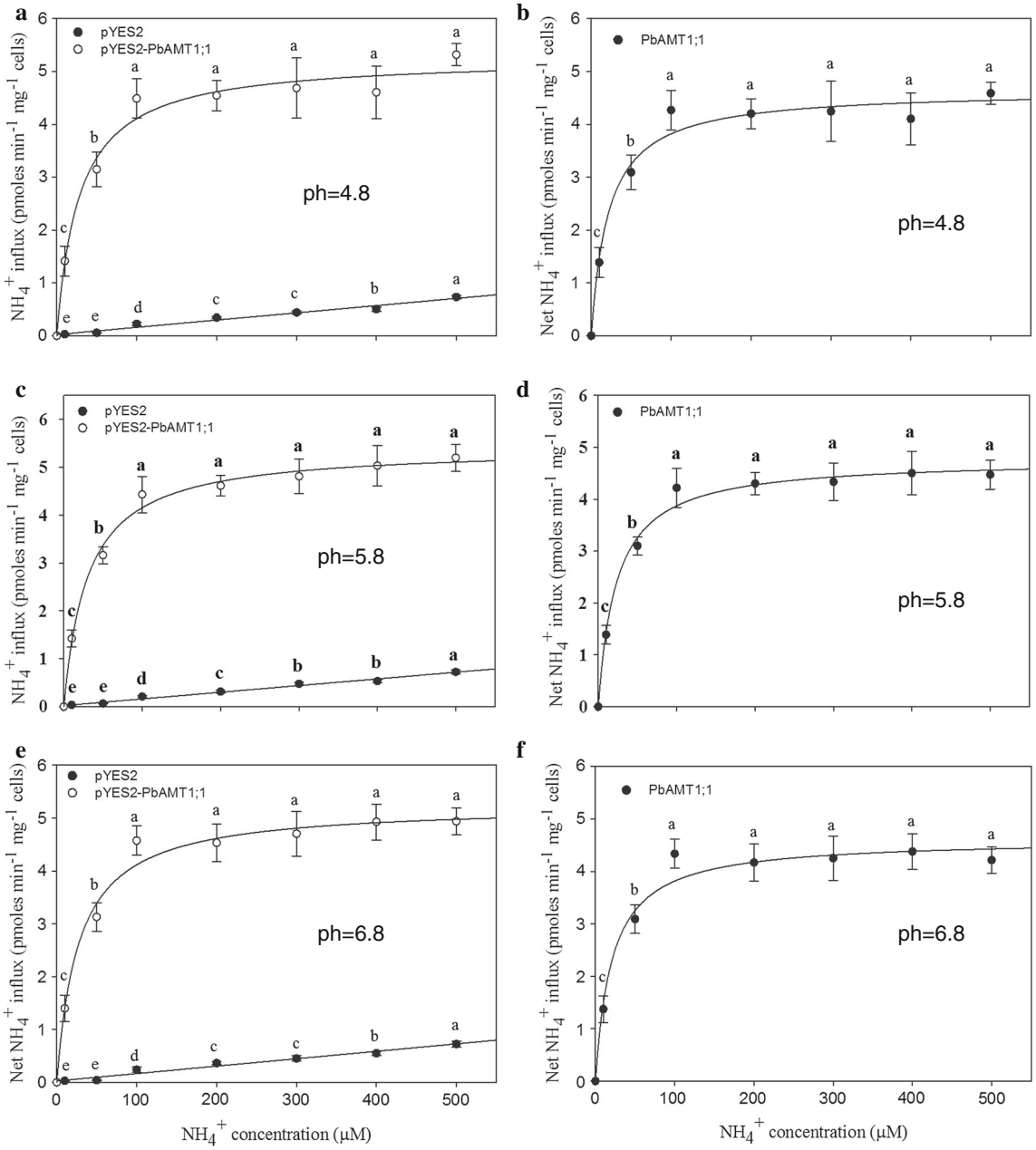

Fig. 9 Kinetic analysis of PbAMT1;1 in transformed yeast in different pH values. Concentration dependent kinetics of $^{15}NH_4^+$ uptake by the yeast strain 31019b transformed with pYES2 alone or pYES2 harboring *PbAMT1;1* ORF. $^{15}NH_4^+$ uptake rates of recombinant yeast cells were determined in response to 10, 50, 100, 200, 300, 400 or 500 μM $^{15}NH_4^+$. Values were measured at 30 min and showed as means with standard error of three replicate experiments. Net $^{15}NH_4^+$ influx mediated by PbAMT1;1 was calculated by subtracting the value of pYES2. Curves were directly fitted to the data for pYES2-PbAMT1;1 and PbAMT1;1 using the Michaelis–Menten equation. A linear curve was used to fit the data for pYES2. **a**, **c** and **e** $^{15}NH_4^+$ uptake by the yeast strain 31019b transformed with pYES2 alone or pYES2 harboring *PbAMT1;1* ORF at different pH value; **b**, **d** and **f** Net $^{15}NH_4^+$ influx mediated by PbAMT1;1 at different pH value

PbAMT1;1 may play a role in stimulating root NH_4^+ uptake under N deficient conditions. In stems and leaves, the *PbAMT1;1* transcript declined during N starvation and did not respond to N resupply (Fig. 4b, c). The *P. betulifolia* belongs to the perennial plants which need to mobilize N from source (roots) to sink tissues (aerial organs), as in the observed results in *Populus trichocarpa* (Couturier et al. 2007). In this kind of plants, the N contents of nutrient storage organs (stems and leaves) did not immediately fluctuate with the concentration of N in the environment. This may be the reason that the *PbAMT1;1* transcript levels in leaves and in stems were less affected

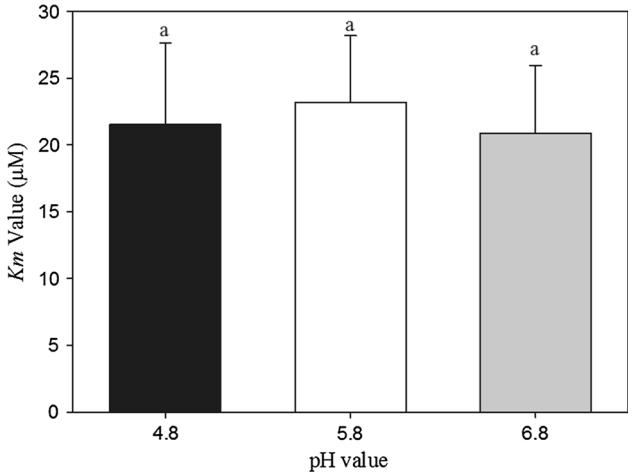

Fig. 10 Effects of proton on $^{15}NH_4^+$ uptake. Net $^{15}NH_4^+$ K_m in yeast cells transformed with *PbAMT1;1* ORF were measured at pH 4.8, 5.8 and 6.8. Each *bar* represents the average data with standard error of three independent experiments. *Different letters* indicate significant differences ($P < 0.05$)

by N levels than in roots. In conclusion, our data provide evidence to enrich the information on *AMT* genes from woody trees. And it will be very interesting to further assess the physiological role of *PbAMT1;1*.

The photorespiratory N cycle generates a large amount of NH_4^+ in leaf mitochondria that is subsequently transported to chloroplasts for reassimilation, implying that the expression of *AMT* genes can be important to ensure the recycling of NH_4^+ during photorespiration. In this study, *PbAMT1;1* exhibited diurnal rhythms with the highest expression level at noonday (Fig. 6). Through this photoperiodicity, we would conclude that *PbAMT1;1* plays a limited role in the transportation of NH_4^+/NH_3 generated by photorespiration. On the other hand, when NH_4^+ concentration is high (10 mM), the mRNA abundant of *PbAMT1;1* increased, which clearly demonstrated that *PbAMT1;1* took part in the NH_4^+ metabolism in leaves.

Couturier et al. (2007) reported that the AMTs might be recruited during senescence. In order to understand whether *PbAMT1;1* participate in this proceed, *P. betulifolia* were treated with two hormone substances, ABA and MeJ, which had the ability to induce senescence in the plant. The results indicated that *PbAMT1;1* may play certain roles in the senescence of plants, because of its transcriptions in leaves were markedly increased under above conditions (Fig. 7). In other cases, *PtrAMT1;5* and *PtrAMT1;6* of poplar were observed expressing in senescing leaves, which functions would be like *PbAMT1;1* (Couturier et al. 2007).

One evaluation index for NH_4^+ affinity, which is characteristic of AMTs, is the K_m value. In fact, the K_m values of AMT1-type proteins show a wide range from a few tenths to a few hundred micromolars because plants have to endure various N soil levels during their life histories. For example, AtAMT1;1 from *Arabidopsis* (Shelden et al. 2001), LjAMT1;1, LjAMT1;2 and LjAMT1;3 from lotus (D'Apuzzo et al. 2004), and LeAMT1;1 from tomato (Ludewig et al. 2002) have lower K_m values, ranging from 0.5 to 40 μM, but are usually listed as high-affinity AMTs. However, some other AMT1-type proteins, such as LeAMT1;2 from tomato (Ludewig et al. 2003), TaAMT1;1 from wheat (Sogaard et al. 2009) and AtAMT1;2 from *Arabidopsis* (Gazzarrini et al. 1999; Neuhäuser et al. 2007), which display higher K_m values (from tens to hundreds), are often classified as low-affinity AMTs. Based on the $^{15}NH_4^+$ absorption experiments with recombinant yeast, the K_m value of PbAMT1;1 was calculated to be approximately 23.2 μM at pH 5.8 (Fig. 9, 10). This result suggested that PbAMT1;1 could be defined as a high-affinity AMT, which may play an important role in NH_4^+ absorption and distribution in the case of N limitation.

Protons are the main factors mediating the NH_4^+ transport function of AMT1 proteins, which have complex regulatory mechanisms. Different *AMT1* genes show distinct responses to the change in external pH. For example, the NH_4^+-induced current of LeAMT1;1 and LeAMT1;2 from tomato were independent of the extracellular pH (Ludewig et al. 2002; Mayer et al. 2006). Here, the K_m of PbAMT1;1 at different pH values had no significant difference which means protons had little effect on the PbAMT1;1 function (Fig. 10). This phenomenon was similar to tomato results (Ludewig et al. 2002; Mayer et al. 2006). However, TaAMT1;1 from wheat (Sogaard et al. 2009) and PvAMT1;1 from bean (Ortiz-Ramirez et al. 2011) were more efficient in the uptake of NH_4^+ under acidic pH conditions. At the same time, the transcription levels of *PbAMT1;1* were also constant under different pH values conditions. Nevertheless, further experimental data would be demanded to identify whether PbAMT1;1 works as an NH_4^+ uniporter or as an NH_3/H^+ co-transporter.

Acknowledgments This work was supported by the Jiangsu Agriculture Science and Technology Innovation Fund of China [CX(12)5033] and the National Natural Sciences Foundation of China (No. 31101529, 31372051, 91125028).

References

Camanẽs G, Cerezo M, Primo-Millo E, Gojon A, García-Agustín P (2007) Ammonium transport and *CitAMT1* expression are regulated by light and sucrose in *Citrus* plants. J Exp Bot 58:2811–2825

Camanẽs G, Cerezo M, Primo-Millo E, Gojon A, García-Agustín P (2009) Ammonium transport and *CitAMT1* expression are regulated by N in *Citrus* plants. Planta 229:331–342

Chang Y, Li H, Cong Y, Lin J, Sheng B (2012) Characterization and expression of a phytochelatin synthase gene in birch-leaf pear (*Pyrus betulifolia* Bunge). Plant Mol Biol Rep 30:1329–1337

Couturier J, Montanini B, Martin F, Brun A, Blaudez D, Chalot M (2007) The expanded family of ammonium transporters in the perennial poplar plant. New Phytol 174:137–150

D'Apuzzo E, Rogato A, Simon-Rosin U, El Alaoui H, Barbulova A, Betti M, Dimou M, Katinakis P, Marquez A, Marini AM, Udvardi MK, Chiurazzi M (2004) Characterization of three functional high-affinity ammonium transporters in *Lotus japonicus* with differential transcriptional regulation spatial expression. Plant Physiol 134:1763–1774

de Castro E, Sigrist CJ, Gattiker A, Bulliard V, Langendijk-Genevaux PS, Gasteiger E, Bairoch A, Hulo N (2006) ScanProsite: detection of PROSITE signature matches and ProRule-associated functional and structural residues in proteins. Nucleic Acids Res 34:w362–w365

Gazzarrini S, Lejay L, Gojon A, Ninnemann O, Frommer WB, von Wirén N (1999) Three functional transporters for constitutive, diurnally regulated, and starvation-induced uptake of ammonium into Arabidopsis roots. Plant Cell 11:937–948

Gu R, Duan F, An X, Zhang F, von Wirén N, Yuan L (2013) Characterization of AMT-mediated high-affinity ammonium uptake in roots of maize (*Zea mays* L.). Plant Cell Physiol 54:1515–1524

Guether M, Neuhäuser B, Balestrini R, Dynowski M, Ludewig U, Bonfante P (2009) A mycorrhizal-Specific ammonium transporter from *Lotus japonicus* acquires nitrogen released by *Arbuscular Mycorrhizal* Fungi. Plant Physiol 150:73–83

He S, Shan W, Kuang J, Xie H, Xiao Y, Lu W, Chen J (2013) Molecular characterization of a stress-response bZIP transcription factor in banana. Plant Cell Tiss Organ Cult 113:173–187

Kaneyoshi J, Wabiko H, Kobayashi S, Tsuchiya T (2001) *Agrobacterium tumefaciens* AKE10-mediated transformation of an Asian pea pear, *Pyrus betulifolia* Bunge: host specificity of bacterial strains. Plant Cell Rep 20:622–628

Kumar A, Silim SN, Okamoto M, Siddiqi MY, Glass AD (2003) Differential expression of three members of the *AMT1* gene family encoding putative high-affinity NH_4^+ transporters in roots of *Oryza sativa* subspecies indica. Plant Cell Environ 26:907–914

Lauter FR, Ninnemann O, Bucher M, Riesmeier JW, Frommer WB (1996) Preferential expression of an ammonium transporter and of two putative nitrate transporters in root hairs of tomato. P Natl Acad Sci USA 93:8139–8144

Loqué D, von Wirén N (2004) Regulatory levels for the transport of ammonium in plant roots. J Exp Bot 55:1293–1305

Ludewig U, von Wirén N, Frommer WB (2002) Uniport of NH_4^+ by the root hair plasma membrane ammonium transporter LeAMT1;1. J Biol Chem 277:13548–13555

Ludewig U, Wilken S, Wu BH, Jost W, Obrdlik P, El Bakkoury M, Marini AM, Andre B, Hamacher T, Boles E, Frommer WB, von Wirén N (2003) Homo- and hetero-oligomerization of ammonium transporter-1 NH_4^+ uniporters. J Biol Chem 278:45603–45610

Marini AM, SoussiBoudekou S, Vissers S, Andre B (1997) A family of ammonium transporters in *Saccharomyces cerevisiae*. Mol Cell Biol 17:4282–4293

Matsumoto K, Chun JP, Tamura F, Kamamoto Y, Tanabe K (2006) Salt tolerance in *Pyrus* species is linked to levels of Na and Cl translocation from roots to leaves. Engei Gakkai Zasshi 75:385–391

Mayer M, Schaaf G, Mouro I, Lopez C, Colin Y, Neumann P, Cartron JP, Ludewig U (2006) Different transport mechanisms in plant and human AMT/Rh-type ammonium transporters. J Gen Physiol 127:133–144

Neuhäuser B, Dynowski M, Mayer M, Ludewig U (2007) Regulation of NH_4^+ transport by essential cross talk between AMT monomers through the carboxyl tails. Plant Physiol 143:1651–1659

Ninnemann O, Jauniaux JC, Frommer WB (1994) Identification of a high-Affinity NH_4^+ transporter from plants. EMBO J 13:3464–3471

Okubo M, Sakuratani T (2000) Effects of sodium chloride on survival and stem elongation of two asian pear rootstock seedlings. Sci Hortic (Amsterdam) 85:85–90

Ortiz-Ramirez C, Mora SI, Trejo J, Pantoja O (2011) PvAMT1;1, a highly selective ammonium transporter that functions as H^+/NH_4^+ symporter. J Biol Chem 286:31113–31122

Salvemini F, Marini AM, Riccio A, Patriarca EJ, Chiurazzi M (2001) Functional characterization of an ammonium transporter gene from *Lotus japonicus*. Gene 270:237–243

Shelden MC, Dong B, de Bruxelles GL, Trevaskis B, Whelan J, Ryan PR, Howitt SM, Udvardi MK (2001) Arabidopsis ammonium transporters, AtAMT1;1 and AtAMT1;2, have different biochemical properties and functional roles. Plant Soil 231:151–160

Sogaard R, Alsterfjord M, MacAulay N, Zeuthen T (2009) Ammonium ion transport by the AMT/Rh homolog TaAMT1;1 is stimulated by acidic pH. Pflug Arch Eur J Phys 458:733–743

Sohlenkamp C, Shelden M, Howitt S, Udvardi M (2000) Characterization of Arabidopsis AtAMT2, a novel ammonium transporter in plants. FEBS Lett 467:273–278

Sonoda Y, Ikeda A, Saiki S, von Wirén N, Yamaya T, Yamaguchi J (2003) Distinct expression and function of three ammonium transporter genes (*OsAMT1;1-1;3*) in rice. Plant Cell Physiol 44:726–734

Tamura K, Peterson D, Peterson N, Stecher G, Nei M, Kumar S (2011) MEGA5: molecular evolutionary genetics analysis using maximum likelihood, evolutionary distance, and maximum parsimony methods. Mol Biol Evol 28:2731–2739

Udvardi MK, Simon-Rosin U, Wood C (2003) Molecular and cellular characterisation of LjAMT2;1, an ammonium transporter from the model legume *Lotus japonicus*. Plant Mol Biol 51:99–108

von Wirén N, Lauter FR, Ninnemann O, Gillissen B, Walch-Liu P, Engels C, Jost W, Frommer WB (2000) Differential regulation of three functional ammonium transporter genes by nitrogen in root hairs and by light in leaves of tomato. Plant J 21:167–175

Wang Y, Zhang C, Jia P, Wang X, Wang W, Dong L (2013) Isolation and expression analysis of three EIN3-like genes in tree peony (*Paeonia suffruticosa*). Plant Cell Tissue Organ Cult 112:181–190

Yamaya T, Suenaga A, Moriya K, Sonoda Y, Ikeda A, von Wirén N, Hayakawa T, Yamaguchi J (2003) Constitutive expression of a novel-type ammonium transporter OsAMT2 in rice plants. Plant Cell Physiol 44:206–211

Yuan LX, Loqué D, Kojima S, Rauch S, Ishiyama K, Inoue E, Takahashi H, von Wirén N (2007) The organization of high-affinity ammonium uptake in Arabidopsis roots depends on the spatial arrangement and biochemical properties of AMT1-type transporters. Plant Cell 19:2636–2652

Yuan LX, Graff L, Loqué D, Kojima S, Tsuchiya YN, Takahashi H, von Wirén N (2009) AtAMT1;4, a pollen-specific high-affinity ammonium transporter of the plasma membrane in *Arabidopsis*. Plant Cell Physiol 50:13–25